INSTITUTE OF PHYSICS PUBLISHING JOURNAL OF PHYSICS B: ATOMIC, MOLECULAR AND OPTICAL PHYSICS

J. Phys. B: At. Mol. Opt. Phys. **36** (2003) 3591–3605 PII: S0953-4075(03)64156-8

Single ionization of calcium by electron impact

Danica Cvejanović and Andrew James Murray

Department of Physics and Astronomy, University of Manchester, Manchester M13 9PL, UK

E-mail: danica@fs3.ph.man.ac.uk and andrew.murray@man.ac.uk

Received 29 May 2003, in final form 9 July 2003
Published 14 August 2003
Online at stacks.iop.org/JPhysB/36/3591

Abstract

Relative cross sections for the single ionization of calcium were measured in the energy range from threshold to 100.7 eV using a time-of-flight ion detection method. Simultaneous detection of the ions from ionization of water molecules was used to monitor and eliminate energy-dependent effects. Present cross sections are normalized at 40 eV using previous experimental data. A comparison is made with existing partial cross sections for Ca^+ as well as total ionization cross sections to highlight the significant difference which exists in the energy shape and magnitude of the cross section maximum.

1. Introduction

Electron impact ionization is one of the basic scattering processes studied from the early days of modern atomic physics, important for both fundamental research in atomic physics and understanding the physics of different types of plasmas and related applications. Experimental efforts have been directed towards measurements of partial and total ionization cross sections by Kieffer and Dunn [1], Märk [2] and, more recently, to gain an insight into atomic structure and ionization dynamics, using differential (e, 2e) coincidence studies (see, for example, [3–5] and references therein). While a wealth of data exists for some atoms, primarily the noble gases, there are relatively few data on alkaline earth atoms. However, due to their orbital structure, alkaline earth atoms present a logical step towards the study of more complex atoms.

Calcium has the same outer orbital configuration as the noble gas helium, yet it is a more complex atom with a larger number of electrons and hence a complex shell structure. It is the smallest closed shell atom which shows the full range of many-electron effects [6]. The energy proximity of the outer 4s shell to the unoccupied 3d orbital has well recognized effects on the excitation and ionization from the 3p shell [6, 7], demonstrating the importance of electron correlations in calcium. Hence, there has been a considerable number of photon impact studies on calcium [6, 8–14], especially concentrating around the removal of a 3p electron from the inner shell. By comparison, there exists a small number of experimental studies of ionization by electron impact and the situation is not much better for theory. This is the case even for ionization of the outermost 4s electron, leading to single ionization into the ground state of the ion. Only a few experiments have been carried out measuring the ionization cross sections

and these were done 30–40 years ago. These studies include experimental partial ionization curves as a function of energy for Ca^+, Ca^{2+}, Ca^{3+} and Ca^{4+} published by Fiquet-Fayard and Lahmani [15] and for Ca^+, Ca^{2+} and Ca^{3+} by Okudaira [16]. Okudaira also gives information on the relative intensities of the differently charged ions and relative efficiency curves for total ion collection. Total absolute cross sections were measured by McFarland [17], Okuno [18] and Vainstein *et al* [19]. Both relative and absolute measurements show significant differences in both the absolute magnitudes and the energy behaviour at energies below 30 eV.

Work by Vainstein *et al* [19] includes calculations using both Born and classical binary approximations. More recently, Roy and Rai [20] have calculated the total ionization cross section using the symmetrical collision model of Vriens [21] along with a Hartee–Fock velocity distribution for the bound electron.

The only electron impact experimental studies in the 3p autoionization region are by Schmitz *et al* [22], Pejčev *et al* [23] and, more recently, Feuerstein *et al* [24]. In the 2p autoionization region measurements have been conducted by Weber *et al* [25] and Chen *et al* [26].

In the laboratory at Manchester work is currently underway on the more detailed (e, 2e) studies on both the ground and $4\,^1P$ laser excited state of calcium. There have been no differential (e, 2e) studies on calcium so far. The work reported here was undertaken in preparation for these experiments and with the aim of obtaining more precise information on the energy behaviour of cross sections for the production of Ca^+ by electron impact. Further, by looking at the region below 30 eV, the structures between 25 and 30 eV previously reported [15, 16] can be studied. The energy region below 30 eV is of interest in the (e, 2e) studies as it corresponds to the low to intermediate energy scattering regime where specific effects, like long and short range correlations, ingoing and outgoing wave distortions, polarization of the target during the collision, post-collision interactions, multiple scattering and exchange effects, are to be expected. The ability to take into account these effects is a very sensitive test for theoretical modelling. In addition, a number of autoionization processes are opening in this energy region, including the excitation and ionization from the 3p shell, which were believed to be responsible for the shape of the cross section previously observed in both single- and total ionization measurements. Since these early experiments [15–19] much more information has been obtained on these autoionizing and Auger states (see, for example, electron impact work by Pejčev *et al* [23], and a photoionization study by Bizau *et al* [6]) and it is useful to make a new assessment on their role in the single ionization of calcium.

Using a time-of-flight method we have simultaneously measured intensities of Ca^+ and H_2O^+ ions produced by electron impact. As ionization cross sections for H_2O^+ are well known, comparison of the two intensities can be used to estimate and eliminate energy-dependent instrumental effects. Data for calcium are normalized at 40 eV to the total ionization cross section using previous Ca^+ partial and total cross sections [16, 18–20]. Comparison with previous data indicates significant differences in both the relative magnitude and shape of the maximum of the partial cross section. This finding also has implications for total cross section values.

2. Experimental details

In the present experiment an energy-unselected electron beam is crossed with an atomic calcium beam emanating from an oven. A simple cylindrical three-element ion detector pulsed appropriately with the electron beam separates different mass ions according to their respective times of flight from the interaction region to the detector. Ions are detected using a channel electron multiplier (CEM) followed by standard counting electronics, as shown in figure 1.

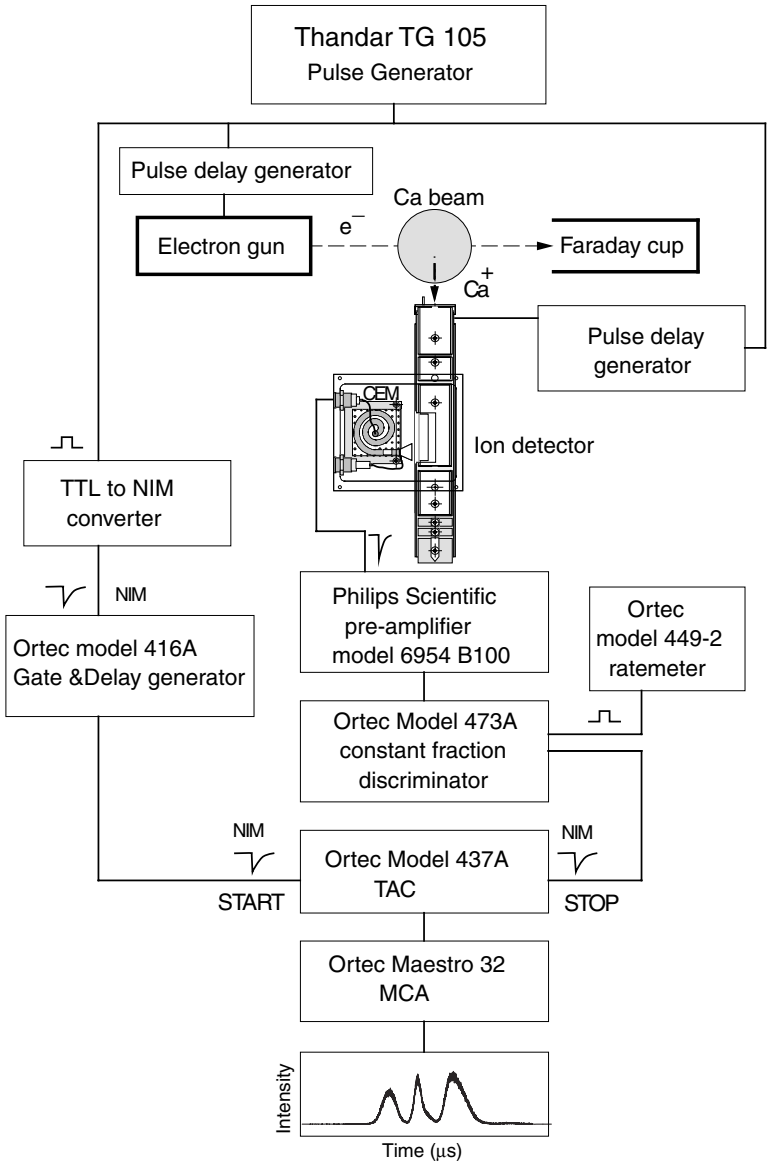

Figure 1. Block diagram of the experiment. For details, see text.

The electron gun consists of a commercial (Agar A054) tungsten filament followed by a Pierce-type extraction stage comprising a grid and an anode. The electron beam is further controlled by a set of two three-element aperture lenses. Two defining apertures and three sets of X–Y deflectors positioned appropriately in the field-free regions control the shape and position of the electron beam with respect to the interaction region. A pair of additional deflectors used only when the gun was pulsed are positioned before the exit aperture. The electron gun was designed for stability over long periods of time and, due to the proximity of the calcium oven, was operated at an average temperature around 80 °C. The energy of the electrons in the incident beam can be varied up to 100 eV with an energy spread of $\approx$700 meV FWHM. The gun can be operated in the continuous or pulsed modes. Typical currents in the

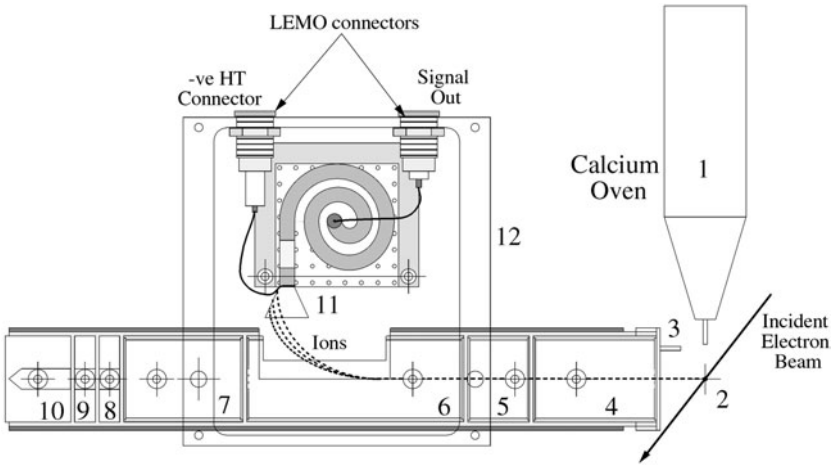

Figure 2. The time-of-flight ion detector, showing the relative position of the detector with respect to the calcium oven (1). The detector used a cylindrical lens and extraction system to pass ions created in the interaction region to the electron multiplier. For details, see the text.

continuous mode measured in the Faraday cup were $\approx 2\ \mu$A. The pulsing was performed by applying appropriate voltages on the grid electrode and the pair of deflectors on the exit of the gun. The power supplies and the pulse delay generators were triggered externally to provide a pulse of variable height, width and delay to both the electron gun and ion detector. Details of the gun and pulsing electronics are described elsewhere [27], while a detailed description of the delay generators was published by Murray and Hammond [28].

The ion detector used for these studies is shown in figure 2. Calcium emitted from the oven (1) was ionized at the interaction region (2) by a pulsed electron beam lasting around 1 μs. The front aperture (3) and extraction electrode (4) of the ion detector were pulsed negative after the electron gun was switched off so as to extract and accelerate ions from the interaction region into the ion detector. The front aperture included a 5 mm long deflector plate which was located on the side nearest the oven. This deflector plate was designed so as to minimize the distortion of the extraction field at the interaction region due to the oven body and nozzle.

The front of the extraction electrode (4) was covered in a fine tungsten gauze so as to provide a uniform extraction field and to allow efficient passage of the ions into the detector. The voltage pulse on the aperture (3) and electrode (4) could be independently varied in amplitude and width, and the pulses could be delayed with respect to each other so as to maximize the extraction yield from the interaction region. Typical voltages on these elements were between -10 and -60 V, with a pulse width ranging from 3 to 30 μs. A cylindrical focusing lens (5) was used to focus ions into the quasi-field-free region (6). Element (6) had a section cut out so that the ions could pass to the CEM located in a shielded housing (12) as shown. The front cone (11) of the CEM was biased at -2.5 kV and the field from this cone penetrated into the quasi-field-free region (6) so as to extract ions into the CEM. The CEM then amplified the signal from the ions and produced a negative going signal at the output, which was passed to the timing and counting electronics shown in figure 1. The cylindrical lens element (7) could be biased positively and this was used to shape the field in region (6) so as to minimize the time spread of the mass-selected ions into the CEM, while maintaining good mass resolution.

The pulse electronics following the CEM consisted of a Phillips Scientific 6954 pre-amplifier located at the vacuum feedthrough, an ORTEC 473A constant fraction

discriminator (CFD) and an ORTEC 449-2 ratemeter. The NIM signal from the 473A CFD was used as the stop signal for the ORTEC 437 TAC, which had been started by the pulse generator and associated electronics, as shown in figure 1.

The design of the ion detector, with the CEM not directly in line with the interaction region, was chosen as it allowed a laser beam to also pass down the centre of the lens elements for the study of ionization from laser-excited targets. The restricted geometry around the interaction region made it difficult to direct the laser beam in any other direction and so it was decided to also make the end of the ion detector a laser beam dump. Hence element (10) was shaped to dissipate the laser beam and reduce optical back-scatter. To prevent electrons or surface ions emitted from the beam dump from passing back down the detector, lens elements (8) and (9) were biased so as to provide a potential barrier to these particles.

The calcium oven consisted of two independently heated parts. The part containing the calcium sample was held at a temperature around 600 °C, while the nozzle incorporating an effusing tube was held at a temperature typically 40 °C higher. The calcium sample obtained from Alfa Aesar (Johnson Matthey) had a stated purity of 99.5%. The design of the oven was optimized for use in (e, 2e) experiments, while details of this design and the oven characteristics are described by Cvejanović and Murray [29]. The calcium beam could be monitored by observation of fluorescence from the laser excitation of calcium via two windows in the side of the vacuum chamber.

In addition to the oven a gas inlet via a tube positioned opposite the oven exit was used to form a gas beam of selected gases, He, Ne, Ar and Kr, at the stage of testing the ion detector and during calibration of the time-of-flight detector. It was also possible to introduce gas into the entire vacuum system via a separate inlet and therefore run the experiment using an evenly distributed sample of atoms, rather than a beam.

All the components: gun, ion detector, calcium oven, Faraday cup, gas inlet and a photon detection system incorporating a lens and optical fibre, were arranged on an optical-type breadboard inside the vacuum chamber, allowing their relative movement and positioning. The atomic beam, electron beam, ion extraction direction and gas inlet were all positioned in the vertical plane and at approximately 45° to each other. The block diagram in figure 1 does not depict their true positioning.

The functioning of the experiment, including pulsing electronics and data accumulation system, is illustrated in figure 1. In brief, a pulse generator (Thandar TG 105) was used to trigger the pulse controlling circuit for the grid and output deflectors of the gun, as well as triggering the delay generator which controlled the pulses to the deflector and extractor of the ion detector. The TG 105 also triggered the start of a time-to-amplitude converter (TAC) via a TTL-to-NIM converter and an Ortec model 416A gate and delay generator. These pulses were delayed appropriately so as to allow the time-of-flight signal to be displayed on the multichannel analyser (MCA), connected to the TAC. The experiment proceeded as follows. The electron gun was pulsed ON for 1 μs at a repetition rate of 11 kHz, and approximately 400 ns after the electrons were switched OFF the ion extractor field was pulsed ON for approximately 5 μs. This extraction pulse accelerated the ions produced by the electron beam towards the ion detector, where they were focused into the CEM using the focusing lens inside the ion detector. The time width, relative time delays and amplitudes of each pulse could be independently adjusted and optimized for optimum performance of the experiment. The signal from the CEM within the ion detector passed to the pre-amplifier and CFD before being passed to the stop input of the 437A TAC. Output from the TAC was fed into an Ortec Maestro32 MCA, where the time spectrum was accumulated and subsequently stored in the memory of a PC.

The base pressure in the chamber during data collection was 2×10^{-6} Torr, and this relatively high pressure meant that ionization of the usual constituents of air was also observed

together with the signal from calcium. For the data presented in this paper the TAC range was chosen so that only the ions detected at the mass number of H_2O^+, N_2^+, O_2^+ and Ca^+ appear in the timing spectrum. The presence of water molecules, for which the ionization cross sections are well known, was utilized to monitor any energy-dependent instrumental effects, as described in detail later.

Calibration of the energy scale was obtained by assuming a Gaussian energy distribution in the incident electron beam and fitting the experimental H_2O^+ intensities in the threshold region to appropriately convoluted theoretical cross sections [30] using the binary-encounter-Bethe (BEB) model [31–33]. For this purpose time spectra were recorded at a fine energy mesh around the ionization threshold of water at 12.61 eV. The resulting correction of 0.7 eV was in line with values which were measured in other experiments, for the same type of filament and the same type of gun. Taking into account possible shifts over longer period of time, the accuracy of the energy scale is estimated to be better than ± 0.2 eV.

Time spectra were recorded several times at 100 eV, including the beginning and the end of a full energy run from the calcium ionization threshold to 100 eV. The ratio of H_2O^+ yield to combined N_2^+ and O_2^+ yield was therefore monitored and was found to be constant over the period over which the measurements were made.

Ionization cross sections for calcium, which we present here, are normalized to existing data at an electron impact energy of 40 eV and in this form are compared with existing partial cross sections for single ionization of calcium and with total ionization cross sections. Details of normalization and errors on the present relative values are discussed in the next section.

3. Results

Time-of-flight spectra isolating H_2O^+, N_2^+, O_2^+ and Ca^+ were recorded at a number of incident electron energies from the Ca ionization threshold at 6.11 eV to an energy of 100.7 eV. Examples of time spectra at four different energies are shown in figure 3. Following a series of measurements over the full range of incident energies, the oven was cooled to eliminate emission of calcium atoms and the time spectra were again recorded at the same energies in the region where ionization of N_2 and O_2 occurs. These results are presented as dots in the figure and appear as somewhat lower curves in the example spectra at 25.7 and 80.7 eV. By recording the difference between the calcium beam being present and the background, the underlying structure from the N_2^+ and O_2^+ in the region of the calcium signal was obtained, permitting a correction to the background signal and allowing an associated error estimate. At 10.7 eV only calcium can be ionized while at 13.7 eV both calcium and water ions were observed. The latter energy is below the ionization threshold for N_2 and O_2 and so these peaks were not observed.

The spectrum shown at 25.7 eV is near the energy region where we detect a maximum in our relative ionization cross section for calcium. At 80.7 eV cross sections for ionization of H_2O, N_2 and O_2 are still increasing, with the maximum for all being around 100 eV. By contrast, the cross section for the ionization of calcium decreases significantly as the energy increases, and so the determination of the intensity of the peaks becomes increasingly important.

Ion intensities represented by the area under the peaks were obtained from a series of time spectra similar to those shown in figure 3, with the background subtracted where applicable. This was the preferred option of analysis as the observed peak shapes were asymmetric and so could not be fitted to a simple function. The asymmetry was especially pronounced at higher impact energies and longer flight times. The asymmetry of the peaks prevented a deconvolution procedure by a multi-peak fitting method which would have been useful as N_2^+ and O_2^+ were not fully resolved from Ca^+.

The present investigation was mainly concerned with obtaining the energy shape of the cross section for single ionization of calcium, as accurately as possible. This included the

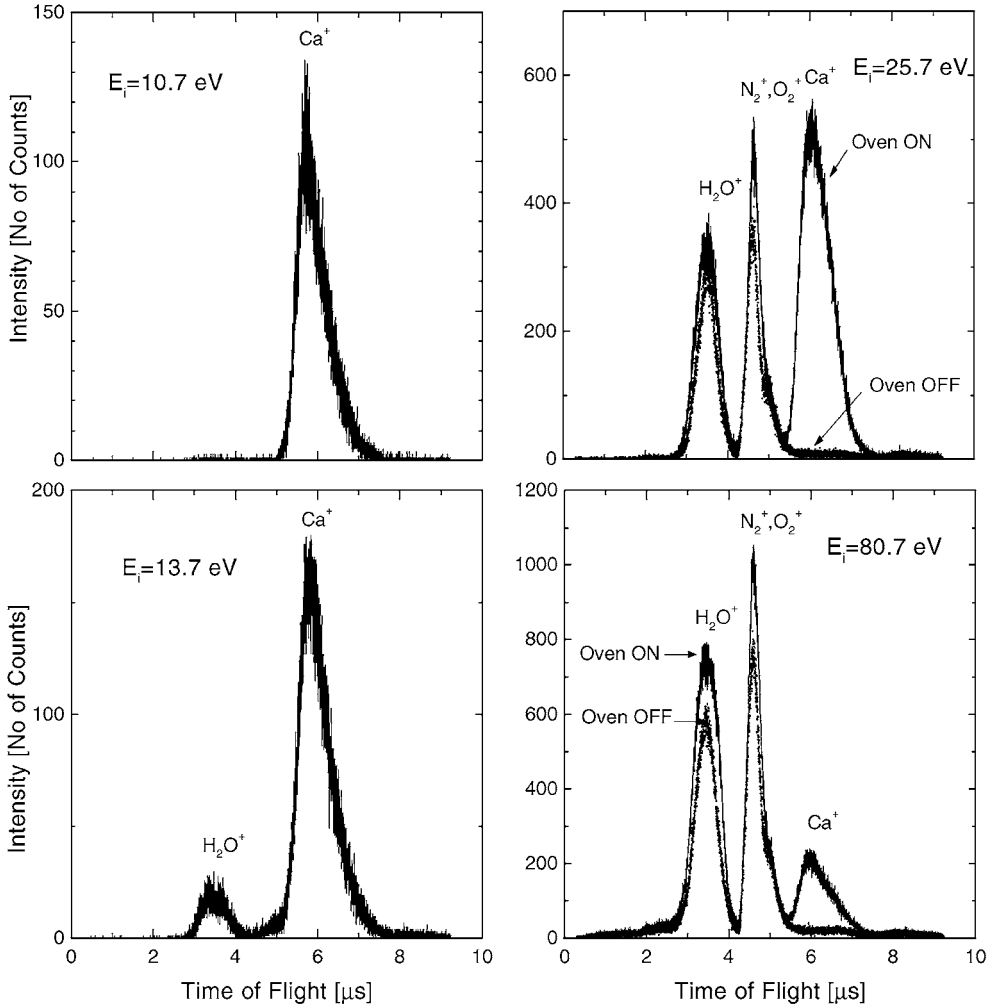

Figure 3. Time-of-flight spectra measured at four different energies illustrating contributing ions and their relative intensities: full curves correspond to measurements with calcium beam, dotted curves at 25.7 and 80.7 eV, i.e. above the N_2 and O_2 ionization threshold, were recorded with no calcium emission.

energy position, magnitude and shape of the maximum as well as the structures in the cross section reported previously [15, 18]. Large differences in these measurements exist between different data sets. Some of the observed differences may be caused by focusing properties in the electron gun in early experiments. Hence it was essential to gain insight into how energy-dependent instrumental effects could influence the present results. This was possible since the existence of H_2O molecules in the background gas could be used to monitor these effects. Ionization cross sections, both experimental and theoretical, exist for water and are in good mutual agreement. Further, the cross section for ionization of water is slowly varying with energy and the shape for the partial cross section, which we measure, and the total cross section is very similar, making it easy to estimate these energy-dependent instrumental effects.

The experimental procedure was as follows. First an estimate of energy-dependent effects was carried out by evaluating H_2O cross sections for the ionization of water from observed

ion intensities. This was achieved by separate comparison with theoretical and experimental data. In this way differences due to the choice of normalization procedure were estimated. Results proved that either approach leads to the same result in the energy range above 17 eV and provided a reliable test for the energy shape of the present results.

The present relative partial cross sections for single ionization of calcium have been indirectly normalized at an electron impact energy of 40 eV using previous experimental values for absolute total ionization cross sections [18, 19] as well as theoretical data [20]. The relative contribution of Ca^{2+} to the total cross section was taken into account by normalizing to the partial cross sections of Okudaira [16]. As the data of Okudaira are themselves relative, a normalization of these was performed to the absolute total cross sections at an energy of 40 eV, where both experimental [18, 19] and theoretical [20] data show good agreement.

3.1. Cross sections for ionization of water and energy-dependent effects in the present experiment

To establish any energy-dependent instrumental effects in the current experiment, H_2O^+ intensities were compared with two existing data sets, a total ionization cross section calculation using a BEB model [31–33] and absolute experimental cross sections for partial ionization published by Straub *et al* [34]. Theoretical BEB cross sections were obtained at the energies used in this experiment from the NIST database [30]. The theoretical BEB data are in good agreement with a number of experimental total ionization data, some of which [34, 35] are shown in figure 4(a), along with the BEB cross sections. Apart from the region near the H_2O ionization threshold, the ratios of theoretical BEB cross section to the present H_2O measurements show only a small variation. Hence a mean value of ratios in the 13.7–100.7 eV energy range was evaluated and this single factor was then used for normalization of H_2O^+ intensities at all energies. Cross sections obtained in this way are shown in figure 4(a). Agreement between the present cross sections and the theoretical results is good throughout the 13.7–100.7 eV energy range, indicating a similar shape of the theoretical BEB and measured partial cross sections. The exception is the energy range between 25 and 40 eV, where the gun focusing conditions were changed. This is seen to affect the intensities by up to 13%. The deviations between theory and the present experimental results for water were used to estimate possible errors on Ca^+ intensities and hence on the measured cross section.

At 13.7 eV close to the H_2O ionization threshold, the water ion intensity is seen to be very small. At lower energies, including energies below the ionization threshold for water, we were not able to check on any possible instrumental effects.

At flight times corresponding to H_2O^+ peaks in figure 3 not all ions created by the electron impact ionization of water were detected, but only an unresolved contribution of H_2O^+, OH^+ and O^+ ions. Hence the measured ion intensities are proportional to the total ionization cross section only below 18 eV, i.e. below the respective onsets for formation of fragment ions OH^+, O^+, H_2^+, H^+ and O^{2+}. At energies above the onset for each fragmentation process the ionization intensity curve is characterized by the appropriate sum of particular partial cross sections rather than the total cross section. Therefore comparison with the sum of absolute partial cross sections for H_2O^+, OH^+ and O^+ reported by Straub *et al* [34] using a time-of-flight method is more appropriate. These authors measured absolute partial cross sections for other ions from H_2O and also report the total cross sections. The total cross sections reported by Straub *et al* are somewhat lower than the theoretical BEB cross sections in the energy region below 100 eV, as can be seen in figure 4(a). Although the total cross section is dominated by H_2O^+ production, some dependence on the choice of normalization can be expected if the total and measured sum of partial cross sections have different energy shapes. It is the shape rather than the absolute value which is important for the estimate of instrumental effects.

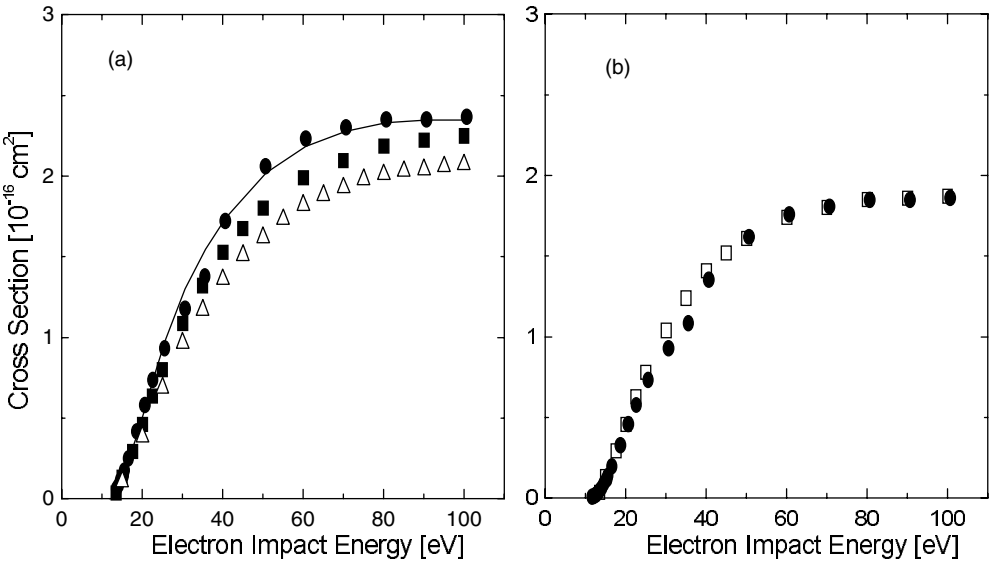

Figure 4. Cross section for ionization of water. (a) Total ionization cross sections: ●, present intensities normalized to theoretical BEB values; ——, theoretical BEB data as obtained from the NIST database [30]; experiments ■, Straub *et al* [34] and △, Djuric *et al* [35]. (b) Partial $H_2O^+ + OH^+ + O^+$ cross sections: ●, present intensities normalized to partial absolute cross sections of Straub *et al* [34] above 50 eV, see the text for details; □, Straub *et al* [34].

Comparison of the present intensities for the dominant ions from H_2O with the experimental results of Straub *et al* [34] leads to similar results at energies above 20 eV, as obtained when BEB calculations were used, while below 20 eV the differences are much larger. The ratios of absolute partial cross sections of Straub *et al* and the present results show a moderate variation at energies between 20 and 40 eV, and at an energy of 50 eV and above the ratios are identical to less than a 1% deviation. Hence the mean value of the experimental ratios from 50.7 to 100.7 eV was used to normalize the present data. These results are shown in figure 4(b) where they are compared with the absolute values of Straub *et al* [34]. The maximum difference between the present data normalized in this way and the data of Straub *et al* is 33% at energies below 17 eV, only 1% at 20.7 eV, and has the same pattern of slow increase from 8% at 22.7 eV to 13% at 35.7 eV, as observed when a comparison was made with the BEB data. At 50.7 eV and all higher energies the difference is less then 1%.

The measurement of the ionization cross section for H_2O described above indicates a good agreement of relative values compared to both theoretical BEB [30] and experimental [34] data at energies above 17 eV. These results can be used to place the ionization cross sections for calcium on an accurate relative scale since both measurements were carried out simultaneously. At lower energies the accuracy of the experimental H_2O data is affected by low H_2O^+ intensities and the correction of data for calcium is less certain. Below the ionization threshold of water no estimate of the instrumental effects was possible.

The only difference between the ionization of water and calcium, which might affect the comparison, is that the H_2O molecules are evenly distributed throughout the vacuum chamber whereas the calcium atoms effuse in the form of a beam from the oven and therefore have a non-uniform spatial distribution. Relevant here is the observation that ion extraction was not limited to a small volume encompassing the interaction region, and therefore small variations due to the spatial profile of the electron beam had no significant effect. In the process of initial

testing and optimization of the experiment the ion detector was moved with respect to the target region and it was observed that the performance was insensitive to this positioning. This could be due to the atomic beam being considerably broader at the interaction region than the electron beam. The atomic beam was monitored by visual observation of fluorescence from laser-excited calcium.

3.2. Cross sections for ionization of calcium

While the main effort in the present work was to establish the energy dependence of partial Ca^+ cross sections, normalization is useful to allow comparison with previous results and to allow discussion of specific features. As the production of Ca^+ ions dominates the total ionization cross sections in the energy range studied here, a comparison with total cross sections is also useful. An approximate normalization was therefore performed of the present Ca^+ intensities. Normalization was also performed on the previously measured relative cross sections of Okudaira [16], both total and partial, and on the Ca^+ ionization efficiency curve of Fiquet-Fayard and Lahmani [15]. All normalizations were performed at 40 eV. This choice of energy is convenient as two existing experimental total ionization cross sections by Okuno [18] and Vainstein *et al* [19], and the theoretical data by Roy and Rai [20], all agree well at 40 eV. A mean cross section value of these three authors was used in the present normalization.

In the first step, the relative total ionization cross section, representing the appropriate sum of partial cross sections for production of Ca^+ and Ca^{2+} published by Okudaira, was normalized at 40 eV using the mean cross section value as discussed above. The same normalization factor determined for the total cross section of Okudaira was then used to normalize his partial cross section for single ionization of calcium. These normalized partial cross section data were then used to rescale the present Ca^+ intensities as well as the experimental data by Fiquet-Fayard and Lahmani, again at 40 eV. In this way the contribution of double ionization was taken into account which, according to Okudaira, amounts to approximately 20% of the total cross section at 40 eV. Partial cross sections for production of Ca^+ obtained by this normalization procedure are shown as full circles in figure 5(a).

The errors affecting our relative data have different origins in different energy regions. At incident energies of 25–40 eV the dominant uncertainty comes from focusing effects in the gun as determined by measurements on water, as discussed above. Directly measured values at energies from 23.7 to 40.7 eV were corrected according to these findings and these corrected values are shown in figure 5(a) as open circles. Statistical errors calculated from repeated measurements with the same focusing conditions on the gun and ion detector were found to be less than $\pm 1\%$ in this energy region.

At 80 eV and above the Ca^+ intensities were significantly lower than neighbouring peaks and so an estimate of the intensities and background was less precise, and the measurements were more affected by statistical fluctuations. The standard deviation of measurements regularly repeated at 100 eV over many hours of data collection was found to be $\pm 6\%$.

Below 20 eV the estimate of instrumental effects based on the ionization of water did depend on whether a comparison was made with theoretical BEB data or experimental data [34]. The energy shape of the present relative cross sections followed the shape predicted by theoretical BEB calculations more closely than the experimental data. A maximum difference of $\pm 33\%$ obtained from comparison with experimental partial cross sections [34] sets the higher confidence limit. Discrepancy between the two sets of experimental data was most likely significantly affected by statistical fluctuations due to the low H_2O^+ intensities near the ionization threshold. Below 13.7 eV it was not possible to determine an appropriate uncertainty.

In figure 5(b) total ionization cross sections are shown in the energy range of the present experiment. These include experimental cross sections by Okuno [18], Vainstein *et al* [19] and

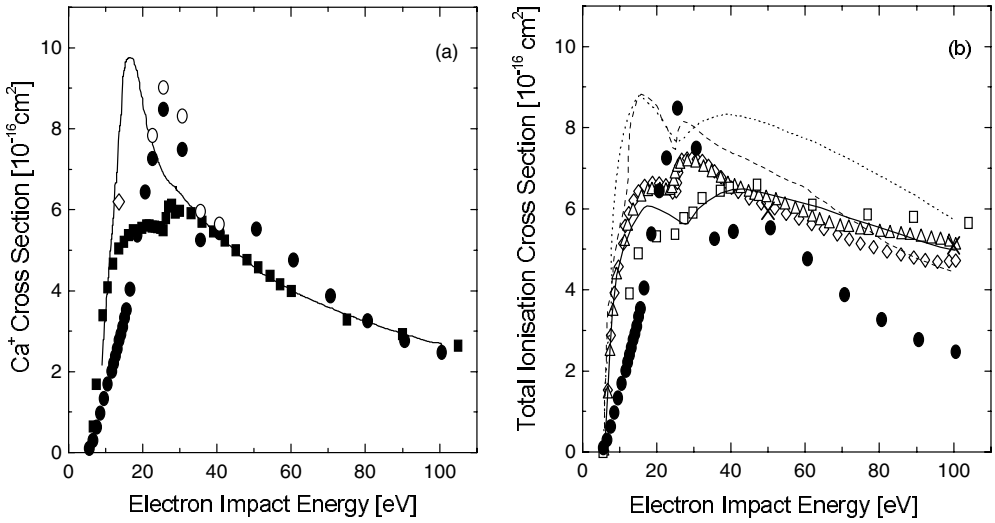

Figure 5. Cross sections for ionization of calcium. (a) Partial Ca^+ cross sections, all normalized at 40 eV: ●, present data from direct measurements; ○, present cross sections corrected by amount determined from measurements on water; ——, Fiquet-Fayard and Lahmani [15]; ■, Okudaira [16]; absolute measurement: ◇, Okuno [18]. (b) Total ionization cross sections, absolute measurements: ×, McFarland [17] divided by two; ◇, Okuno [18]; △, Vainstein *et al* [19]; relative measurements normalized at 40 eV: □, Okudaira [16]; theory: ——, Roy and Rai [20], symmetrical collision model; – – –, Vainstein *et al* [19], Born theory; · · · · · ·, Vainstein *et al* [19], binary encounter theory. ●, Present partial cross sections.

McFarland [17] and the theoretical data by Roy and Rai [20]. Cross sections by McFarland have been divided by a factor of two to permit more convenient presentation. The cross sections for the single ionization of calcium measured here are included in this figure to emphasize the observed difference in energy shape in the energy region dominated by single ionization. Clearly if the peak cross section for single ionization is underestimated so is the total ionization and more experiments as well as theoretical studies are needed to gain more confidence in the description of ionization of calcium in terms of cross sections.

In order to investigate the existence of some fine or additional structures as reported before [15, 16, 18], time spectra were recorded over a fine mesh of energies around 30 eV. These data are shown in figure 6 along with the subset of data covering the full energy range presented in figure 5(a). No significant fine structure was observed in this energy range, although this observation may be limited by the energy spread of the incident electron beam. The measurements over a fine energy mesh were carried out independently of those shown in figure 5(a). The excellent agreement indicates the reproducibility of the experiment for this range of energies.

4. Discussion

A somewhat tentative description of the shape of the observed cross sections is that this is a slowly varying curve with a broad peak centred between 40 and 50 eV. On this curve a much narrower structure with a peak around 25–27 eV can be seen to be superimposed. The onset of the narrower structure starts between 17 and 18 eV. Although all three Ca^+ cross section curves measured by different authors shown in figure 5(a) have very different shapes between

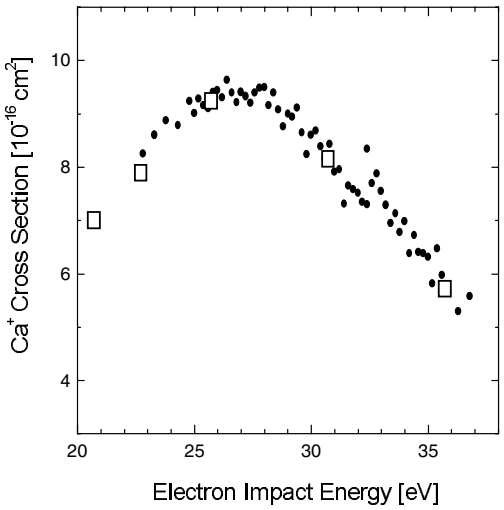

Figure 6. Cross section for ionization of calcium: ···, present measurements around 30 eV performed over a fine mesh of energies; □, subset of present measurements presented in figure 5(a).

30 eV and the ionization threshold, it is interesting to note that each of the authors cite what they consider to be a structure appearing around 25 eV. Hence the existence and location of the structure at 25 eV seems to be more consistently predicted than the different shapes themselves. This composite shape of the cross section in calcium is supported by theoretical data [20] although relative heights observed in the present experiment are significantly different from these predictions. The narrow structure constitutes a dominant part of our cross section in this energy region, indicating the significance of the process which is responsible.

The composite shape of the cross section for the ionization of calcium can be explained in terms of strong excitation of autoionizing states in this atom. This channel of Ca^+ production will be governed by specific excitation and decay mechanisms characteristic for each individual state. For a complete analysis of the contribution to the ionization process due to autoionizing states one would need to know the precise spectroscopic energies, the decay path of these states and their electron impact cross sections. Most of these data are not available for the majority of autoionizing states of interest in the present study. An analysis of the role which autoionization has on Ca^+ production can be discussed in terms of the electron configurations involved. The first contribution comes from the group of states originating from $\cdots 3p^6 nln'l'$ excitation which leads to the first double ionization threshold at 17.8 eV. Excitation of the autoionizing states from this group, apart from any radiative decay to a state of the neutral atom, will always lead to Ca^+ production and will be detected in the present experiment.

A significant process below the double-ionization threshold includes simultaneous excitation and ionization starting at 7.8 eV with excitation of the $\cdots 3p^6 3d\ ^2D_{3/2,5/2}$ states and excitation of the $\cdots 3p^6 4p\ ^2P_{1/2,3/2}$ ionic states at 9.236 and 9.264 eV, respectively. Excited ions would have radiatively decayed prior to detection in our experiment and they will be detected in the same way as ions in the ground state. Excitation of the ^2P states was experimentally studied by Hamdy *et al* [36]. These authors present the emission cross section for the $\lambda = 393.3$ nm line corresponding to the $4\ ^2P_{3/2} \rightarrow 4\ ^2S_{1/2}$ transition and give an estimate of cascade contributions at 40 eV as well as the decay into the lower lying ^2D states. Neither the cascades nor the different decay routes are relevant for the present analyses as the contribution to the Ca^+ production is proportional to the directly measured excitation function. The energy shape, as well as

the magnitude of the emission cross section reported by Hamdy *et al* [36], is relevant for the present data. The emission cross section reported by Hamdy *et al* exhibits an almost linear rise from threshold to approximately 17 eV and is then followed by a flat peak centred around 20 eV. At 17 eV their cross section has a value slightly greater than 1×10^{-16} cm^2 which amounts to approximately 25% of the Ca^+ cross section which we measured. This comparison with only one single excited state in the Ca^+ continuum indicates that the contribution of all the available states of both the neutral atom and single charged ion above the first ionization threshold probably plays a significant role in Ca^+ production. The linear rise observed in the same energy region which continues approximately up to the double-ionization threshold, which is also seen in the present experiment, therefore seems to be a real feature rather than an instrumental effect.

At electron impact energies between 30 and 40 eV the emission cross section of Hamdy *et al* exhibits a broad hump similar to that observed here in the Ca^+ cross section. These authors assign this feature to the opening of a new channel for population of the 4 ^{2}P state of Ca^+ following excitation and possible removal of a 3p electron.

The second group of states which can contribute to the observed Ca^+ production in the present experiment are excited at energies $E \geqslant 24.8$ eV and these originate from the $3p^5 4s^2 nl$ electron configuration, i.e. they correspond to excitation of an electron from the 3p orbital. Unfortunately most of the previous experimental studies of these states have been performed at high electron impact energies. The only ejected electron spectrum in calcium obtained at 30 eV has been published by Pejcev *et al* [23]. These authors give tentative assignments based on the work of Mansfield and Newsom [8] and associate a number of ejected electron peaks with the Ca I dipole-forbidden states. The lowest state at 24.80 eV has been assigned as the $\cdots 3p^5 4s^2 3d\ ^3P_1$ state. This state and several higher ones are observed as dominant ejected electron peaks with energies 18.69 eV for the $^3P_1$ state, at an electron impact energy of 30 eV [23]. Some of these states may have a cross section peaking at threshold, as has been observed in a recent study of ejected electron excitation functions for autoionizing states of Li by Borovik and Krasilinec [37]. Near-threshold, peaks in the cross section would enhance the observed Ca^+ production in the region around 25 eV. Additional contributions to single ionization are expected above the 3p ionization threshold at 34.3 eV. An energy diagram and discussion of the decay of states following a hole creation in the 3p orbital was discussed by Feuerstein *et al* [24] and some of the higher lying of these states may contribute to the single ionization of calcium. Contributions of all the open autoionization channels will be superimposed on the usual direct ionization cross section. In the case of total cross section measurements, contributions from double ionization are added. While these contributions can be attributed to different shapes, the magnitude of the total cross section should always be larger than that for single ionization. As can be seen in figure 5(b) this is not the case in the existing set of cross sections for ionization of calcium due to the normalization procedure. A more precise estimate of single to total ionization cross sections is needed.

Further insight into the disagreement between different experimental data presented in figure 5, as well as the tentative reason for the structured shape proposed above, can be obtained by comparison with the situation in other alkaline earth atoms. The recent discussion of both experimental and theoretical cross sections for single ionization of magnesium published by Boivin and Srivastava [38] points to interesting patterns, which also seem relevant for the ionization of calcium. In magnesium large differences are observed by these authors in both the peak position (up to 8 eV) and magnitude (up to a factor of 1.8) between different sets of experimental data. The early experiments of Okudaira *et al* [39] and Vainstein *et al* [19] show the largest variations, while more recent measurements converge towards the same values in good agreement with theoretical predictions [38]. In view of these results, the differences

between the present and early experiments observed in figure 5 are perhaps not surprising and the need for more experimental and theoretical work is clear.

The shape of the cross section in calcium seems to be somewhere between the shape in magnesium and in barium. While the magnesium cross section exhibits only one single clear peak around 20 eV, barium is characterized with a well developed peak just below 10 eV and a much more dominant and very broad peak centred around 30 eV which is well predicted by theory [40].

Although the above discussion pertains only to the single ionization cross section, the main differences observed below 40 eV will be reflected in the total cross section. A comparison of the present partial and total cross sections in figure 5(b) illustrates this. While the relative magnitudes of the partial and total cross sections can to some extent be affected by the consistency of the normalization procedure, the shape is not very sensitive to this as the total cross section in this energy region is dominated by Ca^+ production.

5. Conclusion

The relative cross sections for single ionization of calcium measured here show significant differences compared to existing data at energies below 40 eV down to the ionization threshold. Differences are observed in both the shape and magnitudes of these partial cross sections.

The present experiment and comparison with previous work indicate that existing experimental and theoretical data do not provide an adequate and consistent description of the ionization of calcium. As has been suggested for magnesium [38], more experimental investigations using different methods are required to elucidate the discrepancies which have been observed.

Acknowledgments

The authors would like to thank Alan Venables and Dave Coleman for excellent technical assistance. The financial support of the Engineering and Physical Science Research Council, UK, is gratefully acknowledged.

References

[1] Kieffer L J and Dunn G H 1966 *Rev. Mod. Phys.* **38** 1
[2] Märk T D 1985 Partial ionization cross sections *Electron Impact Ionization* ed T D Märk and G H Dunn (New York: Springer) chapter 5, p 137
[3] Byron F W and Joachain C J 1989 *Phys. Rep.* **179** 211
[4] McCarthy I E and Weigold E 1995 *Electron Atom Collisions* ed A Dalgarno, P L Knight, F H Read and R N Zare (Cambridge: Cambridge University Press)
[5] Lahmam-Bennani A 1991 *J. Phys. B: At. Mol. Opt. Phys.* **24** 2401
[6] Bizau J M, Gerard P, Wuilleumier F J and Wendin G 1987 *Phys. Rev.* A **36** 1220
[7] Karaziya R I 1981 *Sov. Phys.—Usp.* **24** 775
[8] Mansfield M W D and Newsom G H 1977 *Proc. R. Soc.* **357** 77
[9] Sato Y, Hayaishi T, Itikawa Y, Itoh Y, Murakami J, Nagata T, Sasaki T, Sonntag B, Yagashita A and Yoshino M 1985 *J. Phys. B: At. Mol. Phys.* **18** 225
[10] Ueda K, West J B, Ross K J, Hamdy H, Beyer H J and Kleinpoppen H 1993 *Phys. Rev.* A **48** R863
[11] West J B, Ueda K, Kabachnik N M, Ross K J, Beyer H J and Kleinpoppen H 1996 *Phys. Rev.* A **53** R9
[12] Ueda K, West J B, Ross K J, Kabachnik N M, Beyer H J, Hamdy H and Kleinpoppen H 1997 *J. Phys. B: At. Mol. Opt. Phys.* **30** 2093
[13] Ueda K, Kabachnik N M, West J B, Ross K J, Beyer H J, Hamdy H and Kleinpoppen H 1998 *J. Phys. B: At. Mol. Opt. Phys.* **31** 4331

[14] Beyer H J, West J B, Ross K J and De Fanis A 2000 *J. Phys. B: At. Mol. Opt. Phys.* **33** L767
[15] Fiquet-Fayard F and Lahmani M 1962 *J. Chim. Phys.* **59** 1050
[16] Okudaira S 1970 *J. Phys. Soc. Japan* **29** 409
[17] McFarland R H 1967 *Phys. Rev.* **159** 20
[18] Okuno Y 1971 *J. Phys. Soc. Japan* **31** 1189
[19] Vainstein L A, Ochkur V I, Rakhovskii V I and Stepanov A M 1972 *Sov. Phys.—JETP* **34** 271
[20] Roy B N and Rai D K 1983 *J. Phys. B: At. Mol. Phys.* **16** 4677
[21] Vriens L 1966 *Proc. Phys. Soc.* **89** 13
[22] Schmitz W, Breuckmann B and Mehlhorn W 1976 *J. Phys. B: At. Mol. Phys.* **9** L493
[23] Pejcev V, Ottley T W, Rassi D and Ross K J 1978 *J. Phys. B: At. Mol. Phys.* **11** 531
[24] Feuerstein B, Zatsarinny O I and Mehlhorn W 2000 *J. Phys. B: At. Mol. Opt. Phys.* **33** 1237
[25] Weber W, Breuckmann B, Huster R, Menzel W, Mehlhorn W, Chen M H and Dyall K G 1988 *J. Electron Spectrosc. Relat. Phenom.* **47** 105
[26] Chen M H, Weber W and Mehlhorn W 1989 *J. Electron Spectrosc. Relat. Phenom.* **49** 77
[27] Chandler R and Murray A J 2003 in preparation
[28] Murray A J and Hammond P 1999 *Meas. Sci. Technol.* **10** 225
[29] Cvejanovic D and Murray A J 2002 *Meas. Sci. Technol.* **13** 1482
[30] NIST Database http://physics.nist.gov/PhysRefData/contents.html
[31] Kim Y K and Rudd M E 1994 *Phys. Rev.* A **50** 3954
[32] Hwang W, Kim Y K and Rudd M E 1996 *J. Chem. Phys.* **104** 2956
[33] Kim Y K and Rudd M E 1999 *Comments At. Mol. Phys.* **34** 293
[34] Straub H C, Lindsay B G, Smith K A and Stebbings R F 1998 *J. Chem. Phys.* **108** 109
[35] Djuric N L, Cadez I M and Kurepa M V 1988 *Int. J. Mass. Spectrom. Ion. Processes* **83** R7
[36] Hamdy H, Beyer H J and Kleinpoppen H 1990 *J. Phys. B: At. Mol. Opt. Phys.* **23** 1671
[37] Borovik A A and Krasilinec V N 1999 *J. Phys. B: At. Mol. Opt. Phys.* **32** 1941
[38] Boivin R F and Srivastava S K 1998 *J. Phys. B: At. Mol. Opt. Phys.* **31** 2381
[39] Okudaira S, Kaneko Y and Kanomata I 1970 *J. Phys. Soc. Japan* **28** 1536
[40] Dettmann J M and Karstensen F 1982 *J. Phys. B: At. Mol. Phys.* **15** 287